Eidgenössische Technische Hochschule Zürich
Swiss Federal Institute of Technology Zurich

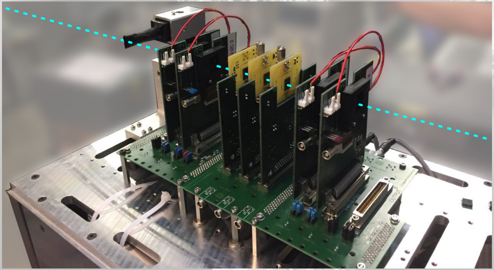

Pulse Height Analysis of 3D pCVD Diamond Detectors

RD42 Meeting - Grenoble 2019

Michael Reichmann

14th November 2019

Table of Contents

Section 1

Introduction

Diamond as Detector Material

- innermost tracking layers $\rightarrow$ highest radiation damage $\mathcal{O}\left(\mathrm{GHz/cm^2}\right)$
- $\rightarrow$ **R&D towards more radiation tolerant detector designs and/or materials**

Diamond as Detector Material

- innermost tracking layers → highest radiation damage $\mathcal{O}\left(\mathrm{GHz/cm^2}\right)$
- → **R&D towards more radiation tolerant detector designs and/or materials**

Diamond as Detector Material:

- advantageous properties
- **after** $1 \cdot 10^{16}\,\mathrm{n/cm^2}$ **the mean drift path in diamond larger than in silicon**

Diamond as Detector Material

- innermost tracking layers → highest radiation damage $\mathcal{O}\left(\mathrm{GHz/cm^2}\right)$
- → **R&D towards more radiation tolerant detector designs and/or materials**

Diamond as Detector Material:

- advantageous properties
- **after $1 \cdot 10^{16}\,\mathrm{n/cm^2}$ the mean drift path in diamond larger than in silicon**

Work at ETH:

- investigate signals and radiation tolerance in various detector designs:
  - Pad Detectors → whole diamond as single cell readout
  - Pixel Detectors → diamond sensor on pixel readout chip
  - 3D Pixel Detectors → 3D diamond detector on pixel readout chip

Diamond as Detector Material

- innermost tracking layers $\rightarrow$ highest radiation damage $\mathcal{O}\left(\mathrm{GHz/cm^2}\right)$
- $\rightarrow$ **R&D towards more radiation tolerant detector designs and/or materials**

Diamond as Detector Material:

- advantageous properties
- **after $1 \cdot 10^{16}\,\mathrm{n/cm^2}$ the mean drift path in diamond larger than in silicon**

Work at ETH:

- investigate signals and radiation tolerance in various detector designs:
  - Pad Detectors
  - Pixel Detectors
  - **3D Pixel Detectors** $\rightarrow$ this talk

Detectors

	II6-A2	**II6-B6**
manufacturer	II-VI Inc.	II-VI Inc.
diamond type	poly-crystal	poly-crystal
size	$\sim$4 mm $\times$ 4 mm	$\sim$4 mm $\times$ 4 mm
thickness	$\sim$500 µm	455 µm
irradiation	none	none
construction	summer 2016	summer 2017
3D drilling	Oxford	Oxford
3D cell size	150 µm $\times$ 100 µm	50 µm $\times$ 50 µm
columns	20 $\times$ 30 **(600)**	60 $\times$ 62 **(3720)**
pixel chip	PSI46digV2.1respin (CMS)	PSI46digV2.1respin (CMS)
pixel pitch	150 µm $\times$ 100 µm	150 µm $\times$ 100 µm
ganged cells	none	2 $\times$ 3 (6 cells)
bump & wire bonding	Princeton	Princeton

Table: 3D Pixel Detector Properties.

Detectors

	II6-A2	**II6-B6**
manufacturer	II-VI Inc.	II-VI Inc.
diamond type	poly-crystal	poly-crystal
size	$\sim$4 mm $\times$ 4 mm	$\sim$4 mm $\times$ 4 mm
thickness	$\sim$500 µm	455 µm
irradiation	none	none
construction	summer 2016	summer 2017
3D drilling	Oxford	Oxford
3D cell size	150 µm $\times$ 100 µm	50 µm $\times$ 50 µm
columns	20 $\times$ 30 **(600)**	60 $\times$ 62 **(3720)**
pixel chip	PSI46digV2.1respin (CMS)	PSI46digV2.1respin (CMS)
pixel pitch	150 µm $\times$ 100 µm	150 µm $\times$ 100 µm
ganged cells	none	2 $\times$ 3 (6 cells)
bump & wire bonding	Princeton	Princeton

Table: 3D Pixel Detector Properties.

- II6-A2 broke in October 2016 (chip malfunctioned) $\rightarrow$ successful re-bonding
- II6-B6 has long history of breaking ...

Measurements

	Oct 16	May 17	Aug 17	Sep 18	Oct 18	Oct 18
place	PSI	PSI	PSI	CERN	CERN	PSI
II6-A2	✓	✓	✓	✓	✓	✓
II6-B6	✗	✗	✓	✗	✓	✓

Table: 3D Pixel Detector Measurements.

- at PSI: scanning particle rate, bias voltage, rise time and incident angle
- at CERN: high resolution studies at different voltages

Measurements

	Oct 16	May 17	Aug 17	Sep 18	Oct 18	Oct 18
place	PSI	PSI	PSI	CERN	CERN	PSI
II6-A2	✓	✓	✓	✓	✓	✓
II6-B6	✗	✗	✓	✗	✓	✓

Table: 3D Pixel Detector Measurements.

- at PSI: scanning particle rate, bias voltage, rise time and incident angle
- at CERN: high resolution studies at different voltages

History of II6-B2:

- 06/2017 - sensor processing and detector fabrication
- 08/2017 - first measurement $\rightarrow$ high efficiency $\rightarrow$ pedestal in pulse height
- 04/2018 - several pixels malfunction $\rightarrow$ re-bump-bonding to new chip
- 06/2018 - sensor detaches while shipping $\rightarrow$ re-bump-bonding, fixate with silguard
- 10/2018 - at PSI: efficiency worsens and sensor detaches again
- 11/2019 - reprocessing and new bump bonding

Section 2

3D Pixel Detector

Working Principle

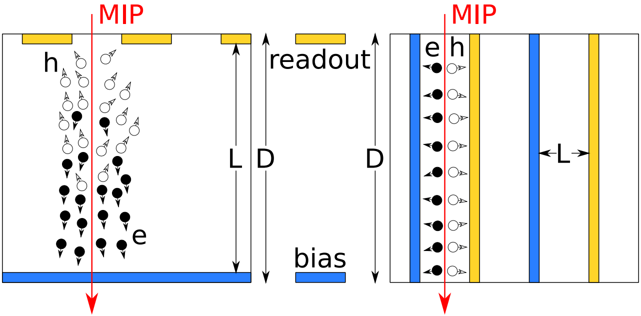

- after large radiation fluence all detectors become trap limited
- bias and readout electrode inside detector material
- same thickness D $\rightarrow$ same amount of induced charge $\rightarrow$ shorter drift distance L
- **increase collected charge in detectors with limited mean drift path (Schubweg)**

Bump Bonding

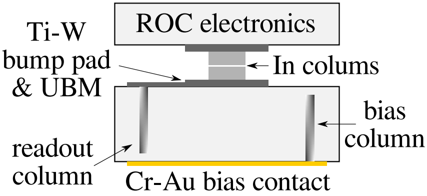

(a) Bump bond schematics

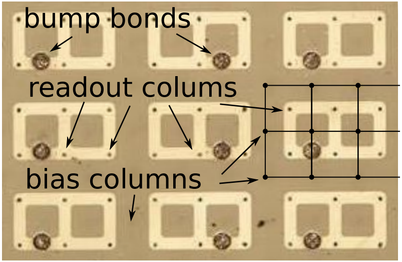

(b) 3 × 2 bump pads

- electrodes (columns) drilled with femto-second laser
- connection to bias and readout with surface metallisation
- ganging of cells to match pixel pitch of readout-chip (ROC)
- small gap (∼15 μm) to the surface to avoid a high voltage break-through

Section 3

Reprocessing of II6-B6 in Fall 2019

Reprocessing B6

- surface cleaning and RIE (Reactive Ion Etching) at OSU
- bias metallisation at OSU
- old mask was rotated...

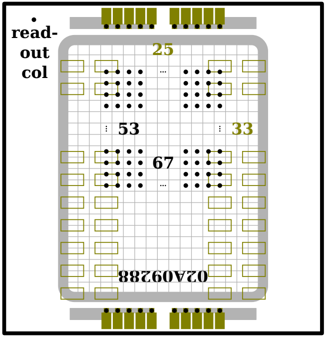

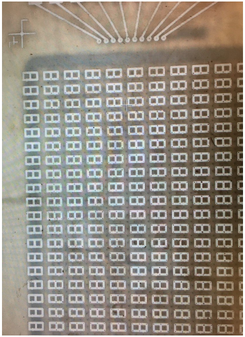

- new mask design including non drilled area for surface detector
- readout metallisation with new mask by Bert in Princeton
- bump-bonding very soon and then test at DESY

Reprocessing B6

- surface cleaning and RIE (Reactive Ion Etching) at OSU
- bias metallisation at OSU
- old mask was rotated...

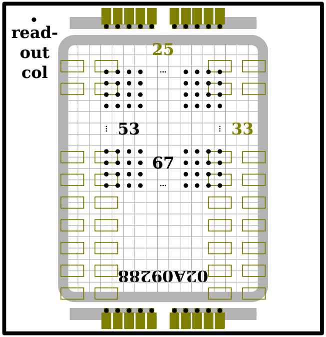

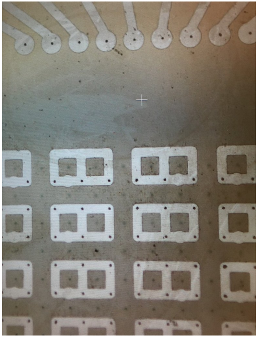

- new mask design including non drilled area for surface detector
- readout metallisation with new mask by Bert in Princeton
- bump-bonding very soon and then test at DESY

Reprocessing B6

- surface cleaning and RIE (Reactive Ion Etching) at OSU
- bias metallisation at OSU
- old mask was rotated...

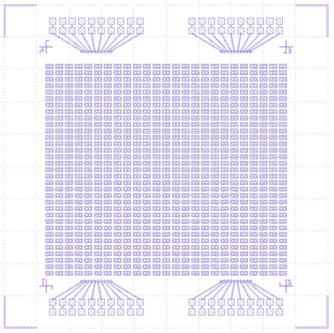

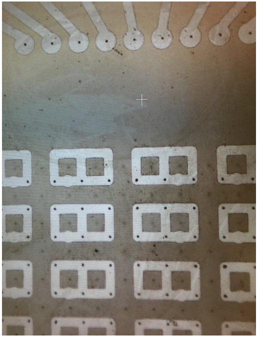

- new mask design including non drilled area for surface detector
- readout metallisation with new mask by Bert in Princeton
- bump-bonding very soon and then test at DESY

Section 4

Setup at PSI

Pixel Telescope

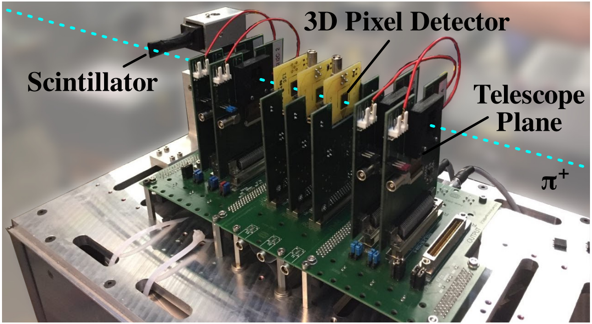

Figure: modular ETH beam telescope in pixel configuration

- 4 tracking planes → trigger (fast-OR) → adjustable area (max 8 mm × 7.8 mm)
- up to 3 DUT planes (any digital pixel detector)
- scintillator for precise trigger timing → $\mathcal{O}$ (1 ns)

Schematic Setup

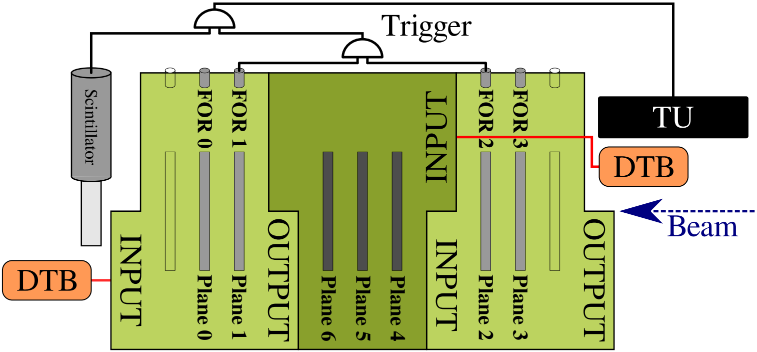

- independent telescope module for DUTs (dark green)
- scintillator → precise trigger timing of $\mathcal{O}(1\,\mathrm{ns})$
- Trigger Unit (TU) → strongly simplifying setup
- global trigger → (Plane 1 AND Plane 2) AND Scintillator

Section 5

Pulse Height Calibration

Pixel Unit Cell

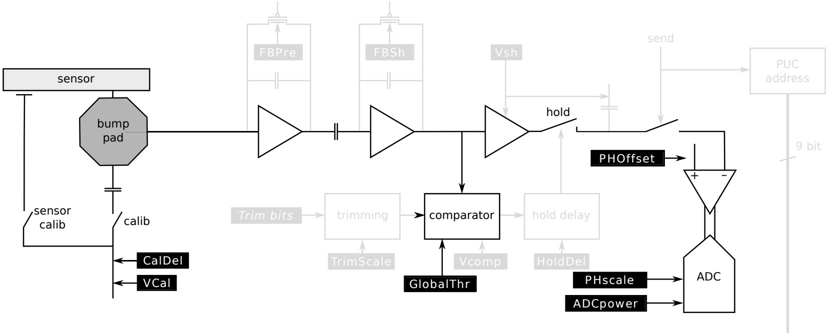

- inject calibration signal ($\sim$vcal) through sensor into same circuit as real signals
- shaping, amplification, threshold check
- set amplification offset
- convert to 8 bit adc value with adjustable scale $\rightarrow$ readout

ADC Calibration

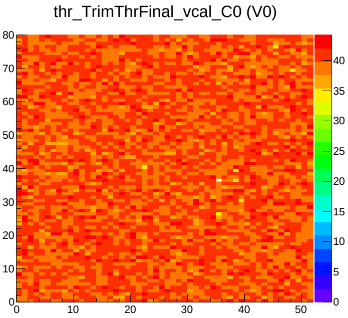

(a) Threshold Map.

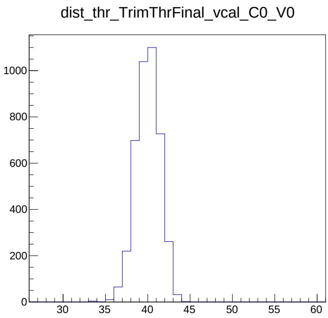

(b) Threshold Distribution.

- trim all pixels to the same threshold

ADC Calibration

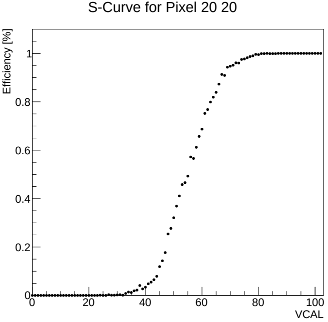

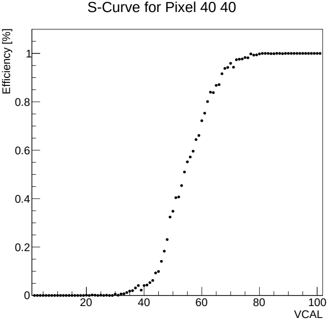

- trim all pixels to the same threshold
- means pixel start to become efficient at the tuned threshold

ADC Calibration

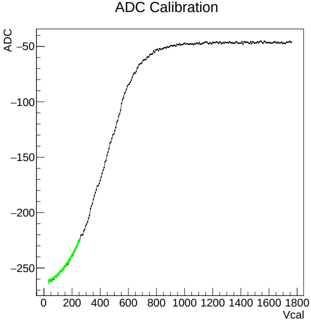

Figure: ADC calibration for single pixel.

- measure adc values for calibration pulses with different vcal
- adc follows error function and saturates for high vcal

ADC Calibration

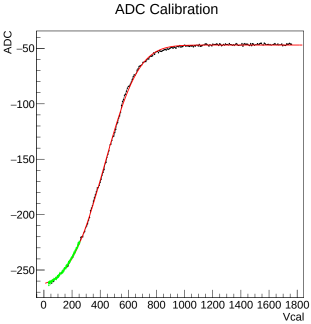

Figure: ADC calibration for single pixel with error function fit.

- measure adc values for calibration pulses with different vcal
- adc follows error function and saturates for high vcal
- fit every pixel and save fit parameters
- adjust adc offset and range with DACs of the chip

ADC Calibration - Temperature Dependence

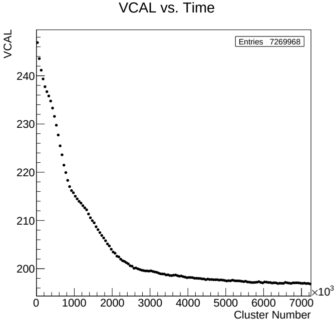

Figure: Read back VCAL inducing test-pulses with VCAL 200.

- readout chip heats up quite significantly while being in use
- adc calibration strongly temperature dependent
- inducing test pulses with VCAL 200 at room temperature
  - converting the measured ADC back to VCAL using the calibration
  - VCAL only approaches the correct value after the chip reaches the correct temperature
- $\rightarrow$ always perform calibration after heating up the chip!

Vcal Calibration (Silicon)

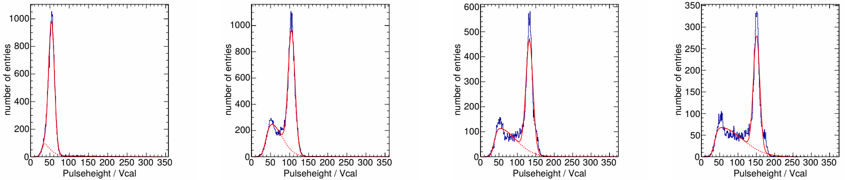

(a) Zn target. (b) Mo target. (a) Ag target. (b) Sn target.

- measure energy spectra of K_α lines of four metal targets using ADC-calibration

Vcal Calibration (Silicon)

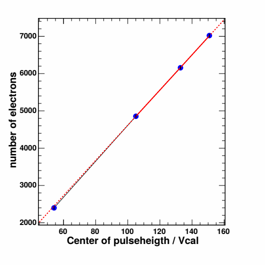

Figure: Vcal Calibration.

- measure energy spectra of K_α lines of four metal targets using ADC-calibration
- linear dependence of energy [e] and vcal
- fit K_α points with straight line (similar for each chip)
- impossible to do calibration with diamond (energy too low)

Vcal Calibration (Silicon)

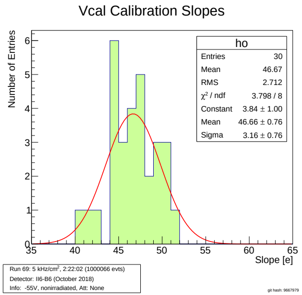

(a) Vcal slopes.

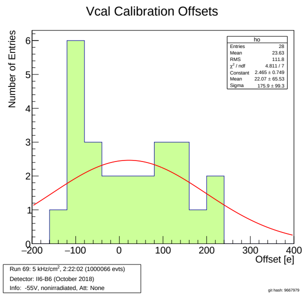

(b) Vcal offsets.

- measure energy spectra of K_α lines of four metal targets using ADC-calibration
- linear dependence of energy [e] and vcal
- fit K_α points with straight line (similar for each chip)
- impossible to do calibration with diamond (energy too low)
  - use general values from silicon: $\mathrm{e} = 46.5 \cdot \mathit{vcal}$

Section 6

Analysis

Cuts

Cut	Excluded Events
event range	first minute of the run due to various beam conditions
beam interruptions	during rate changes of the beam due to beam interruption
aligned	DUT and Telescope are not aligned (event-wise)
trigger phase	Chip trigger timing is incorrect
tracks	not all telescope planes have exactly one cluster
chi2 (x/y)	badly fit tracks (>50 % quantile)
track slope (x/y)	large angles of the tracks (>2 deg)
rhit	large DUT residual (>100 mm)
pixel mask	noisy pixels
fiducial	not in selected (fiducial) area of the DUT

Table: Analysis cut flow.

- cuts applied in order of the table
- largest contribution usually by chi2, tracks and fiducial cuts

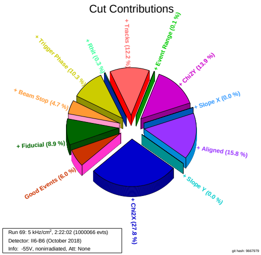

Section 7

Results

PSI - August 2017

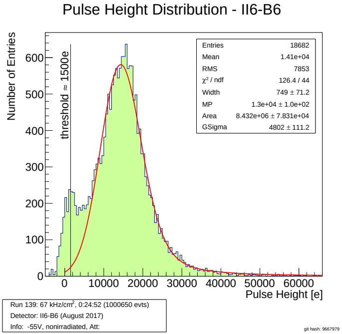

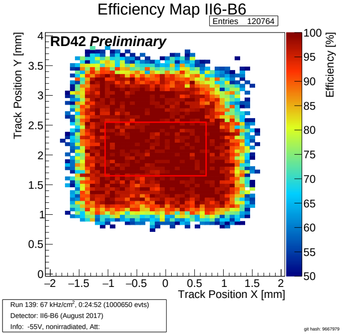

- pulse height looks OK, but “pedestal” of unknown origin (cannot be real)
  - cannot be remeasured, since the ROC was exchanged
- Langau MPV: 13 500 e
- uniform efficiency

PSI - August 2017

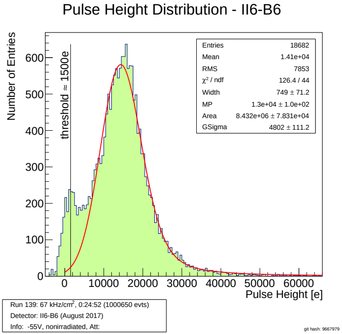

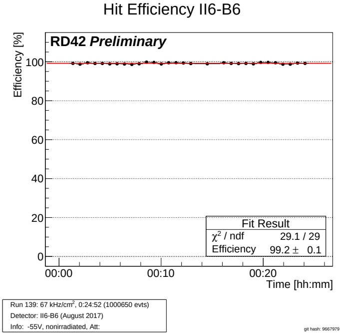

- pulse height looks OK, but “pedestal” of unknown origin (cannot be real)
  - cannot be remeasured, since the ROC was exchanged
- Langau MPV: 13 500 e
- uniform efficiency
- high efficiency of $(99.2 \pm 0.1)\,\%$

PSI - Oct 2018

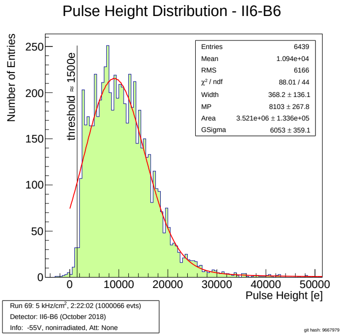

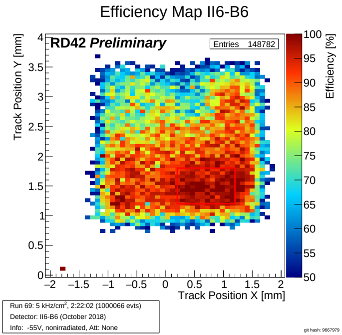

- left part of pulse height distribution not understood
- Langau MPV: 8000 e
- efficiency much less uniform → already loose bumps?

PSI - Oct 2018

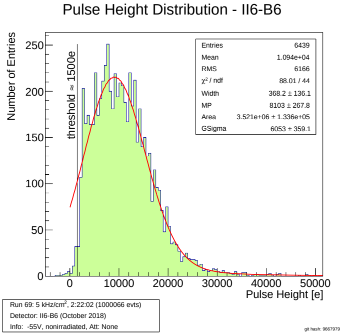

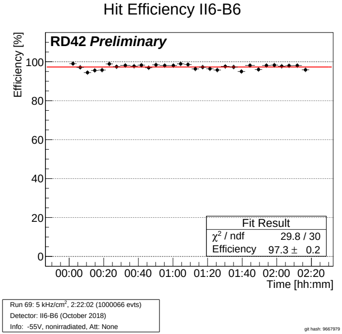

- left part of pulse height distribution not understood
- Langau MPV: 8000 e
- efficiency much less uniform → already loose bumps?
- lower efficiency of $(97.3 \pm 0.2)\,\%$

CERN - Oct 2018

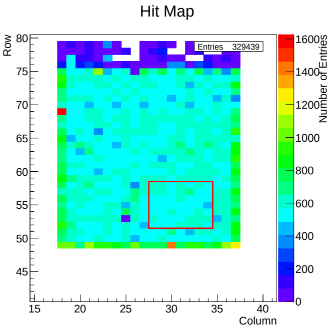

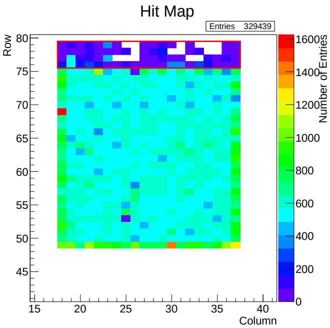

- tried different calibrations of the chip
- using the same region as at PSI
- also small region with 3D cells without bump-bonding (rows 76-79)

CERN - Oct 2018 (0)

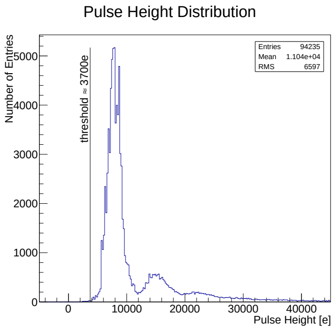

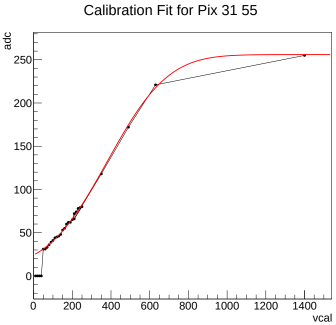

- calibration on the bench for single plane, operation with three planes
- error fit to demonstrate the calibration for a single pixel
- calibration clearly wrong

CERN - Oct 2018 (1)

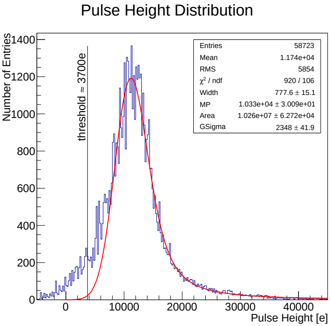

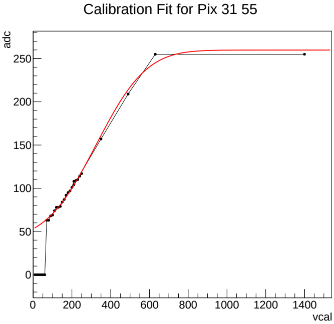

- calibration in situ, operation with three planes
- weird low side of the distribution

CERN - Oct 2018 (2)

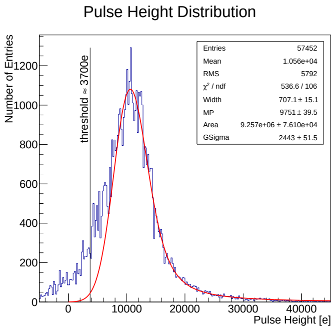

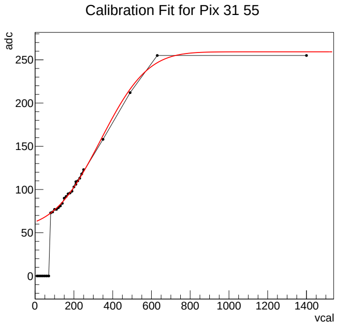

- re-calibration in situ, operation with three planes
- gives very similar result
- all calibrations in situ very similar.

CERN - Oct 2018 (3)

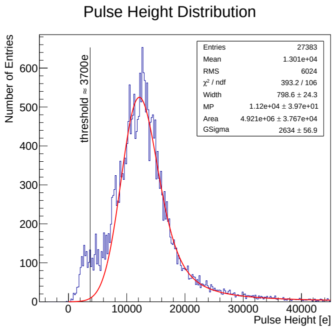

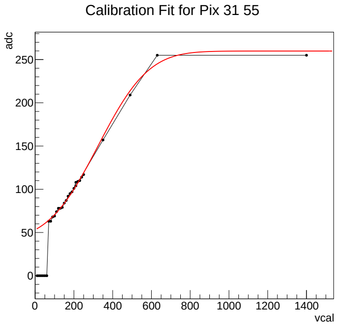

- calibration in situ, operation with single plane
- distribution looks very well, but still small negative contribution
- → small/negative signals can be related to small/degraded analogue signals...

CERN - Oct 2018 (4)

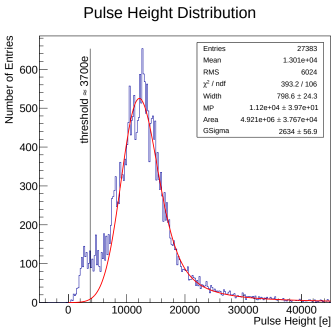

(a) Area with 3D columns.

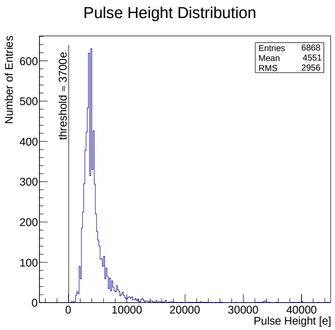

(b) Area without 3D columns.

- comparison between regions with and without 3D columns

Section 8

Conclusion

Conclusion

- many different measurement of both 3D diamond detectors
  - start analyse more data!
- X-ray pulse height calibration can hardly be performed on diamond
  - need to use estimate from silicon
- in situ adc calibration is quite constant
- almost all pulse height distribution show nonphysical low contribution
  - possible reason: degraded analogue signals from chip to readout

Del Fin

Section 9

Backup

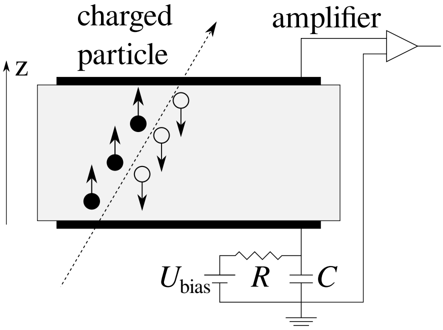

(a) Detector Schematics

(b) 15 cm ⌀ pCVD Diamond Wafer

- detectors operated as ionisation chambers
- metallisation on both sides
- poly-crystals produced in large wafers